Supplementary Figures

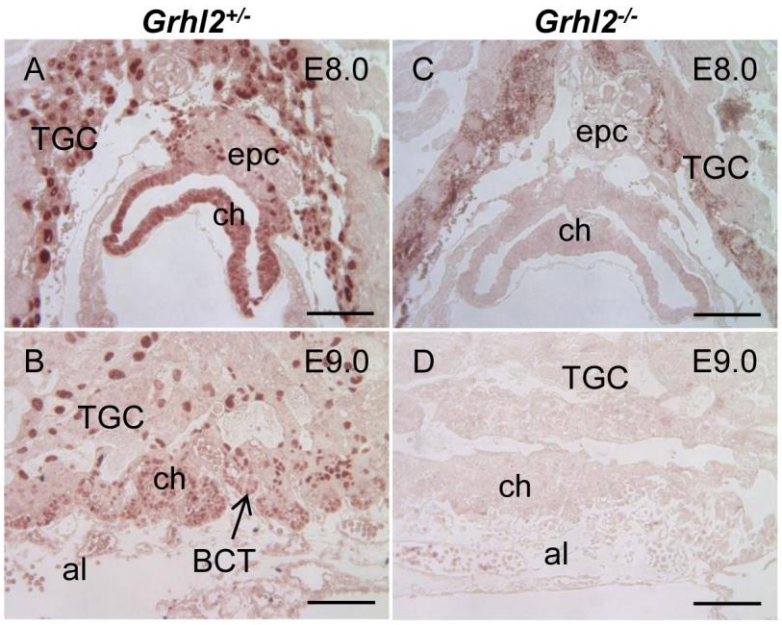

Fig. S1. GRHL2 expression pattern in the mouse placenta. GRHL2 expression analysis in control *Grhl2*$^{+/-}$ placentas at E8.0 (A) and E9.0 (B) showed that GRHL2 was highly expressed in the primary and secondary trophoblast giant cells (TGC). Moreover, GRHL2 expression was detected in the chorion (ch) at E8.0 and became restricted to the BCT cells at E9.0 (B, arrow). In contrast, no GRHL2 staining was observed in *Grhl2*$^{-/-}$ placentas at E8.0 (C) and E9.0 (D). al, allantois; epc, ectoplacental cone. Scale bar: 100 µm. Related to Fig. 1.

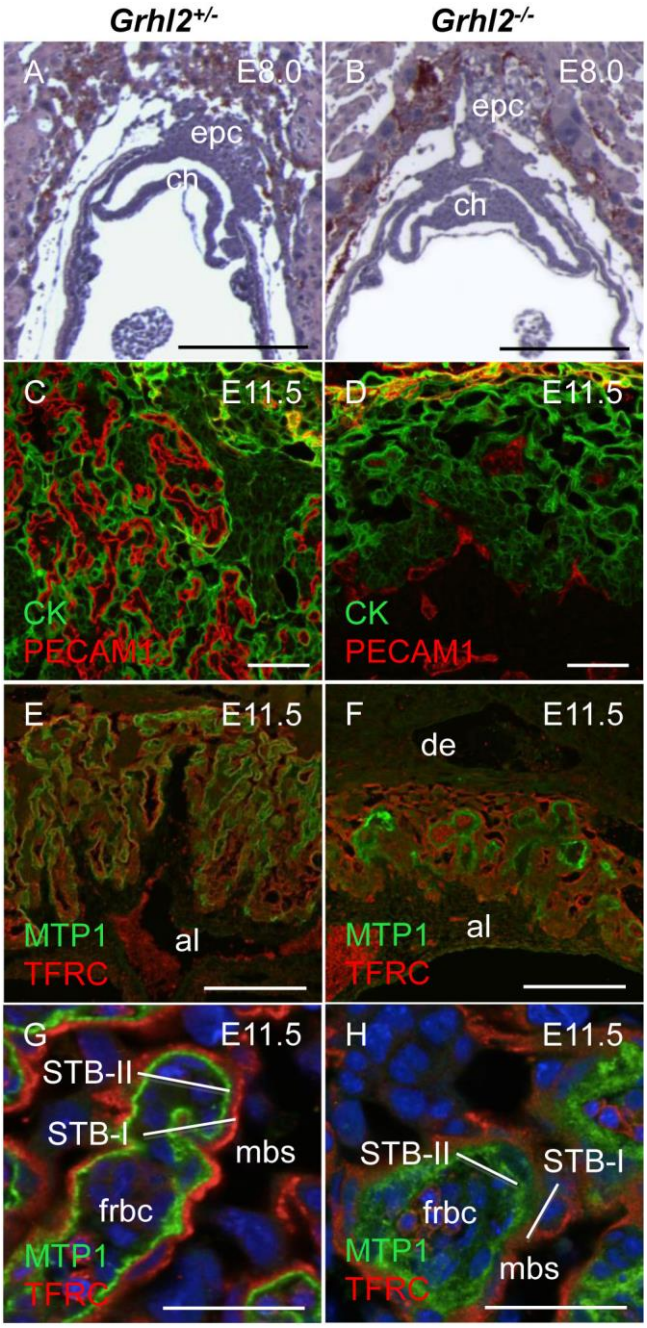

Fig. S2. Defective vascularization and trophoblast branching in *Grhl2*$^{-/-}$ placentas. (A,B) Comparison of H&E-stained sections of control *Grhl2*$^{+/-}$ and mutant placentas showed a normal placenta development of *Grhl2*$^{-/-}$ embryos until E8.0. Scale bar: 250 µm. (C,D) Immunofluorescence staining of pan-cytokeratin (CK, green) and PECAM1 (red) at E11.5 revealed that *Grhl2*$^{-/-}$ placentas exhibited remarkably fewer fetal blood vessels in the labyrinth and a compact labyrinth structure compared to controls. Scale bar: 75 µm. (E-H) Labeling of the syncytiotrophoblast (STB) layers at E11.5 by transferrin receptor (TFRC, red, STB layer I (STB-I)) and ferroportin (MTP1, green, STB layer II (STB-II)) staining (E11.5 low magnification: E, F, scale bar: 250 µm; high magnification: G, H, scale bar: 50 µm) demonstrated that trophoblast branching was initiated in *Grhl2*$^{-/-}$ placentas, but that progression of labyrinth formation was disturbed, resulting in few and simple trophoblast branches (F) compared to the complex STB network in controls (E). Higher magnification revealed an increased thickness of STB-II in mutants indicated by a broadened staining of MTP1 (H) when compared to controls (G). al, allantois; ch, chorion; de, epc, ectoplacental cone; decidua; frbc, fetal red blood cells; mbs, maternal blood sinus. Related to Fig. 2.

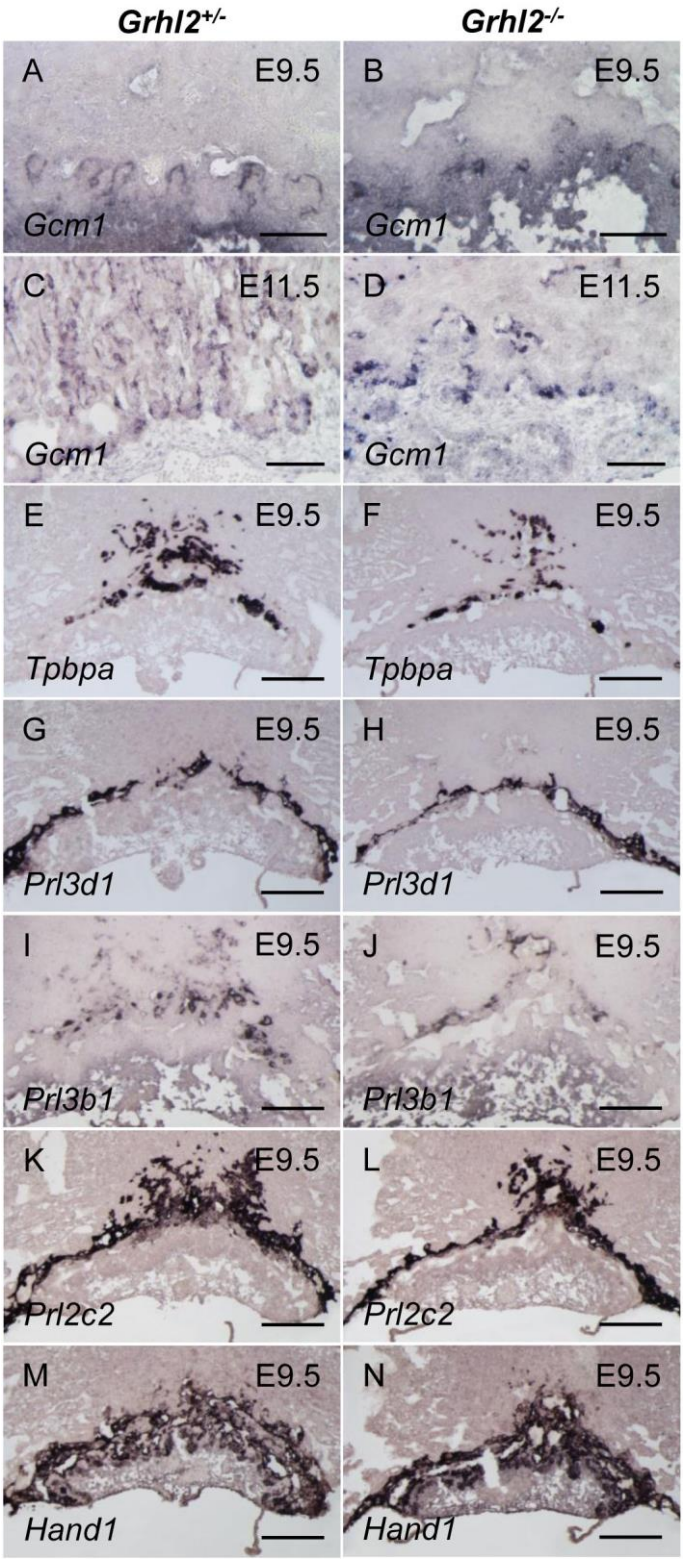

Fig. S3. Spongiotrophoblast, TGC and initiation marker for labyrinthal morphogenesis were maintained in *Grhl2*$^{-/-}$ placentas. (A-D) Branch point labeling in the chorionic trophoblast layer by *Gcm1 in situ* hybridization (ISH) showed that *Gcm1* expression was present at the sites of branch point initiation in *Grhl2*$^{-/-}$ placentas at E9.5, but the amount of *Gcm1*-positive branching initiation sites was markedly reduced (B) compared to controls (A). *Gcm1* staining at E11.5 (C,D) detecting branch points in the labyrinth revealed a massively disturbed branching morphogenesis in *Grhl2*$^{-/-}$ placentas (D). Scale bar: 100 µm. (E,F) Staining of the spongiotrophoblast marker *Tpbpa* by ISH revealed that *Tpbpa* was present in *Grhl2*$^{-/-}$ placentas at E9.5. (G-N) Giant cell markers *Prl3d1* (G,H), *Prl3b1* (I,J), *Prl2c2* (K,L) and *Hand1* (M,N) showed no substantial expression difference at E9.5. Scale bars of E9.5 placentas: 250 µm. Related to Fig. 2.

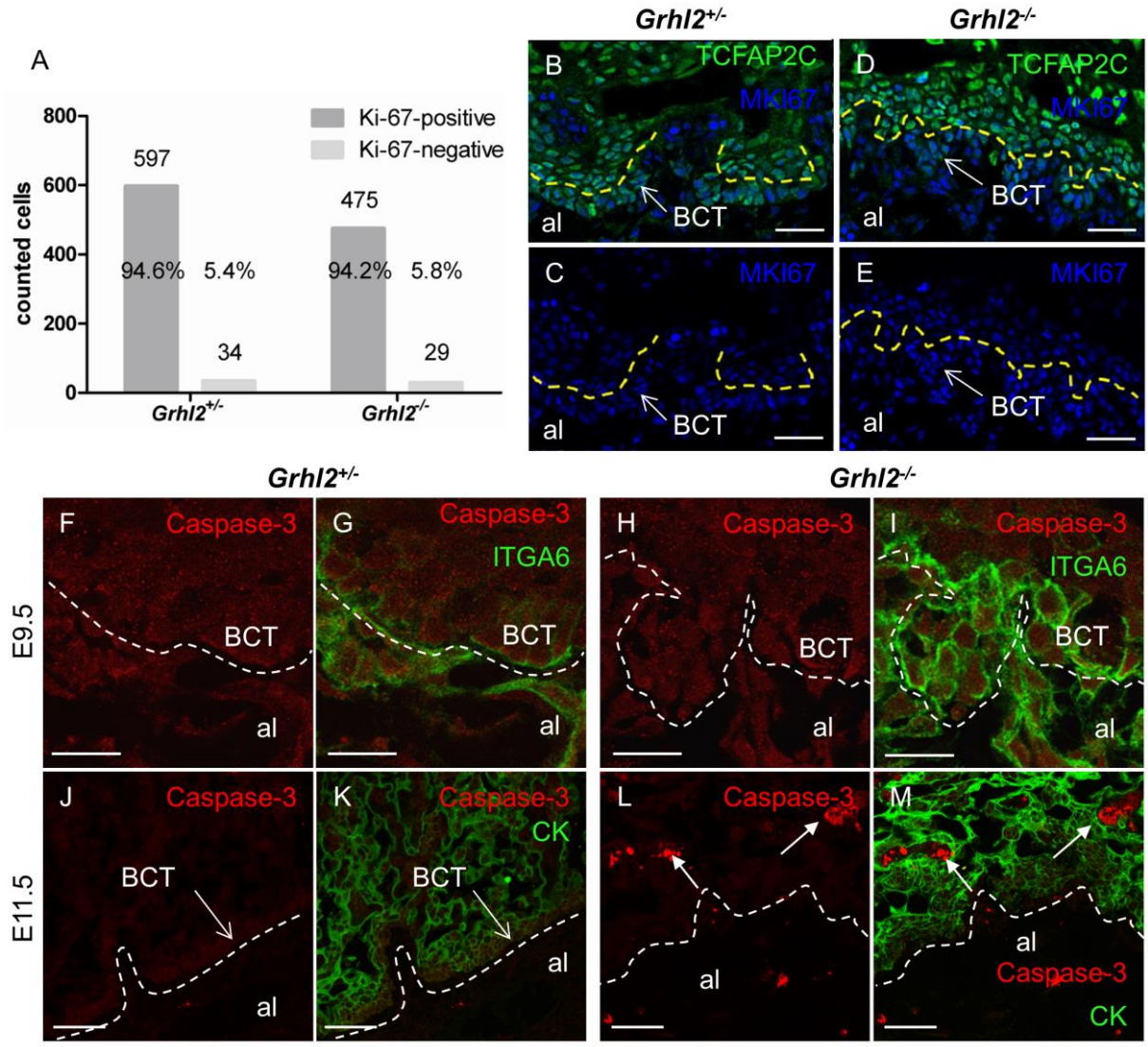

Fig. S4. Analysis of cell proliferation and apoptosis in control and *Grhl2*$^{-/-}$ placentas. (A-E) Analysis of cell proliferation via Ki-67 immunofluorescence staining showed no proliferation differences of the basal chorionic trophoblast (BCT) cells in controls and *Grhl2* mutants at E9.5 (96.6% in *Grhl2*$^{+/-}$ versus 96.4% in *Grhl2*$^{-/-}$ placentas). The yellow dashed line separates the BCT cells from overlying trophoblast cell layers. Scale bar: 100 µm. (F-M) Cell apoptosis was analyzed by active caspase-3 immunostaining (red). Co-staining with the epithelial basolateral marker integrin alpha 6 (ITGA6, green, E9.5, G,I) or with pan-cytokeratin (CK, green, E11.5, K,M) facilitated the identification of BCT cells. We found no evidence for trophoblast apoptosis in control (F,G) and *Grhl2*$^{-/-}$ placentas (H,I) at E9.5. At E11.5, several fetal blood cells were apoptotic in *Grhl2*$^{-/-}$ placentas (L,M, arrows) likely due to secondary effects originating from defective feto-maternal exchange. The white dashed lines mark the border between epithelial trophoblasts and allantois (al). Scale bar E9.5: 100 µm. Scale bar E11.5: 250 µm. Related to Fig. 2.

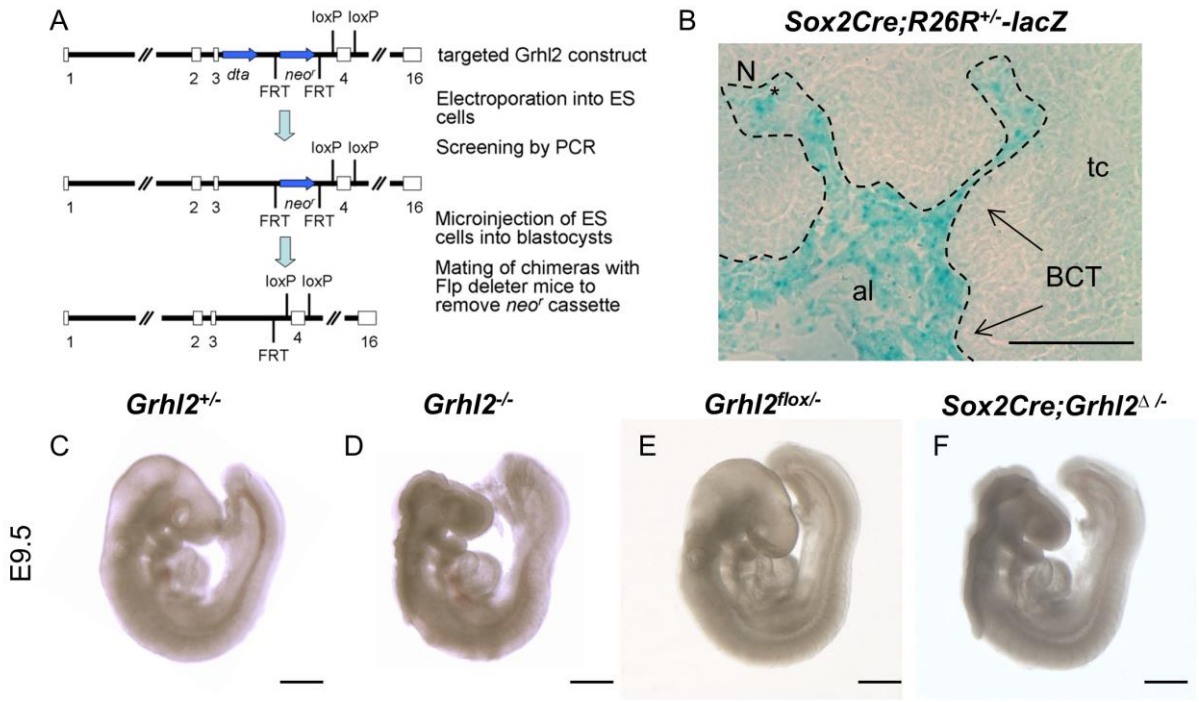

Fig. S5. Selective inactivation of *Grhl2* in epiblast-derived tissues. (A) Targeting strategy for generating a conditional *Grhl2* allele. The targeted *Grhl2* construct is depicted on top. Open boxes represent exons. The diphtheria toxin A (*dta*) and neomycin resistance (*neo*') sequences are indicated by blue arrows. *Neo*^{r} was flanked by two FRT sites, exon 4 of *Grhl2* by two loxP sites. Depicted in the middle is the targeted *Grhl2* allele after electroporation and insertion into the genome of ES cells by homologous recombination. Random integration was reduced through the presence of the *dta* cassette at the 5' end of the construct. Identification of ES cells carrying the targeted *Grhl2* allele was achieved by G418 selection and subsequent PCR. The bottom diagram represents the final floxed *Grhl2* allele after crossing of chimeric mice with Flp deleter mice to remove *neo*^{r} sequences. (B) *Sox2Cre*-mediated activation of β-galactosidase in *R26R* mice. Female *R26R* mice were bred with male *Sox2Cre* mice, and placentas of E9.5 pups were analyzed via X-gal histochemical staining. At E9.5 allantoic mesenchymal cells derived from the epiblast appeared in blue color, including fetal blood vessels (asterisks) arising from the allantois (al). In contrast, all trophectoderm-derived cell types including the basal chorionic trophoblast (BCT) cells remained unstained, indicating that *Sox2Cre*-mediated recombination occurred specifically in the epiblast-derived tissues. The dashed line marks the boundary between trophoblast compartment and allantois. tc, trophoblast cell(s). Scale bar: 100 µm. (C-F) Images of E9.5 littermate control embryos (C: *Grhl2*$^{+/-}$; E: *Grhl2*$^{flox/-}$), *Grhl2*$^{-/-}$ embryos (D) and *Sox2Cre;Grhl2*$^{\Delta/-}$ embryos (F). *Grhl2*$^{-/-}$ and *Sox2Cre;Grhl2*$^{\Delta/-}$ embryos exhibited an identical phenotype including split-face malformations, exencephaly plus anterior and lumbosacral spina bifida. Scale bar: 500 µm. Related to Fig. 3.

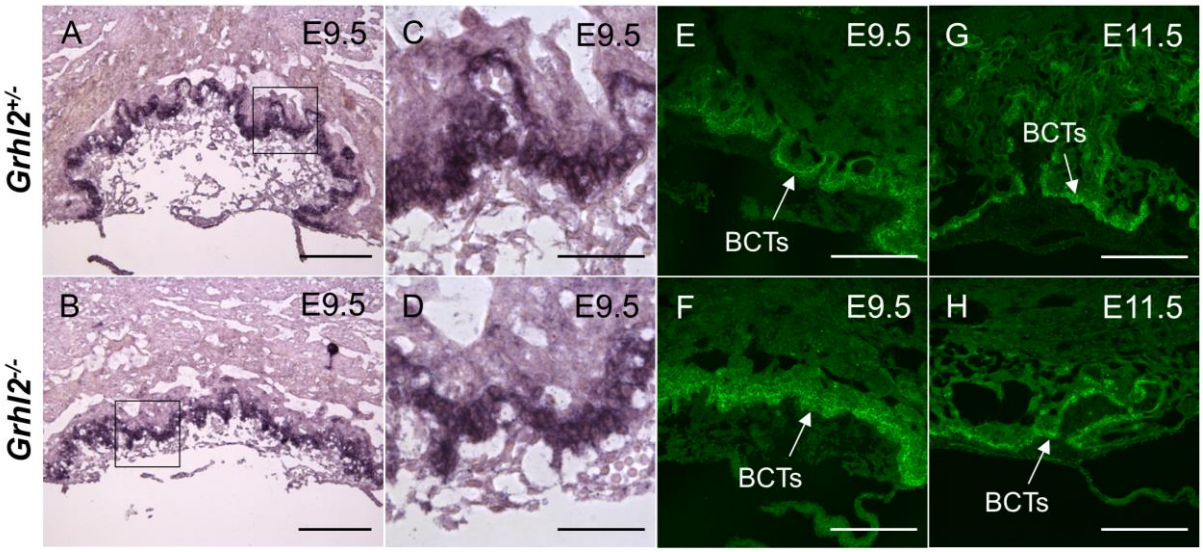

Fig. S6. *Cldn4* expression in the BCT cells of *Grhl2*$^{-/-}$ placentas is unchanged on RNA and protein level. (A-D) *In situ* hybridization on E9.5 placenta sections showed the same expression intensity for *Cldn4* in BCT cells of *Grhl2* mutant (B,D) and control placentas (A,C). Boxed regions in A,B are magnified in C,D. Scale bars A,B: 250 µm. Scale bars C,D: 75 µm. (E-H) Immunofluorescence staining revealed strong expression of CLDN4 in the BCT cells in control *Grhl2*$^{+/-}$ (E,G) as wells as in *Grhl2*$^{-/-}$ placentas (F,H) compared to overlying trophoblast cell layers, respectively. CLDN4 expression levels in BCT cells of *Grhl2*$^{-/-}$ placentas are comparable to that of controls at E9.5 (E,F) as well as E11.5 (G,H). Scale bars: 250 µm. Related to Fig. 6.

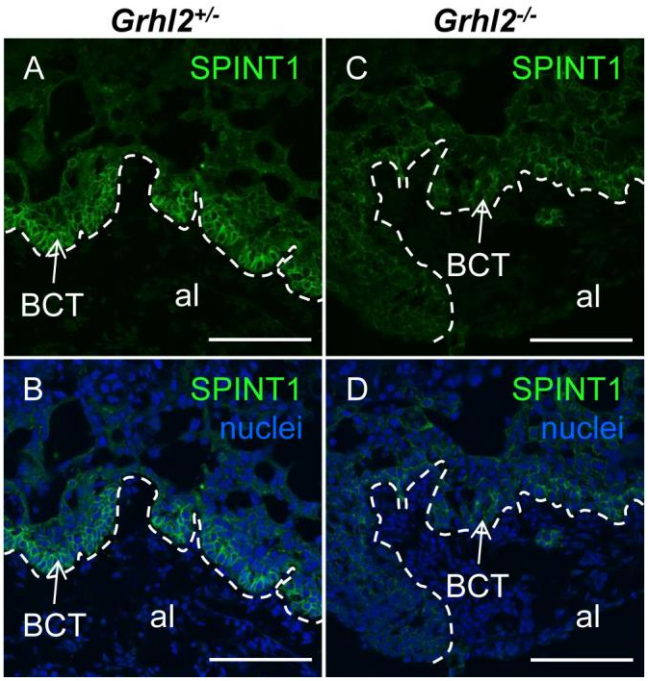

Fig. S7. GRHL2 regulated SPINT1 expression in the BCT cells of murine placentas and was necessary for normal arrangement of trophoblast epithelia. *Grhl2* ablation in murine placentas resulted in a strong downregulation of SPINT1 specifically in the BCT cells (C,D) when compared to controls (A,B) at E9.5. The weak expression of SPINT1 in the overlying trophoblast cells was maintained (C,D). Scale bar: 250 µm. Related to Fig. 6.

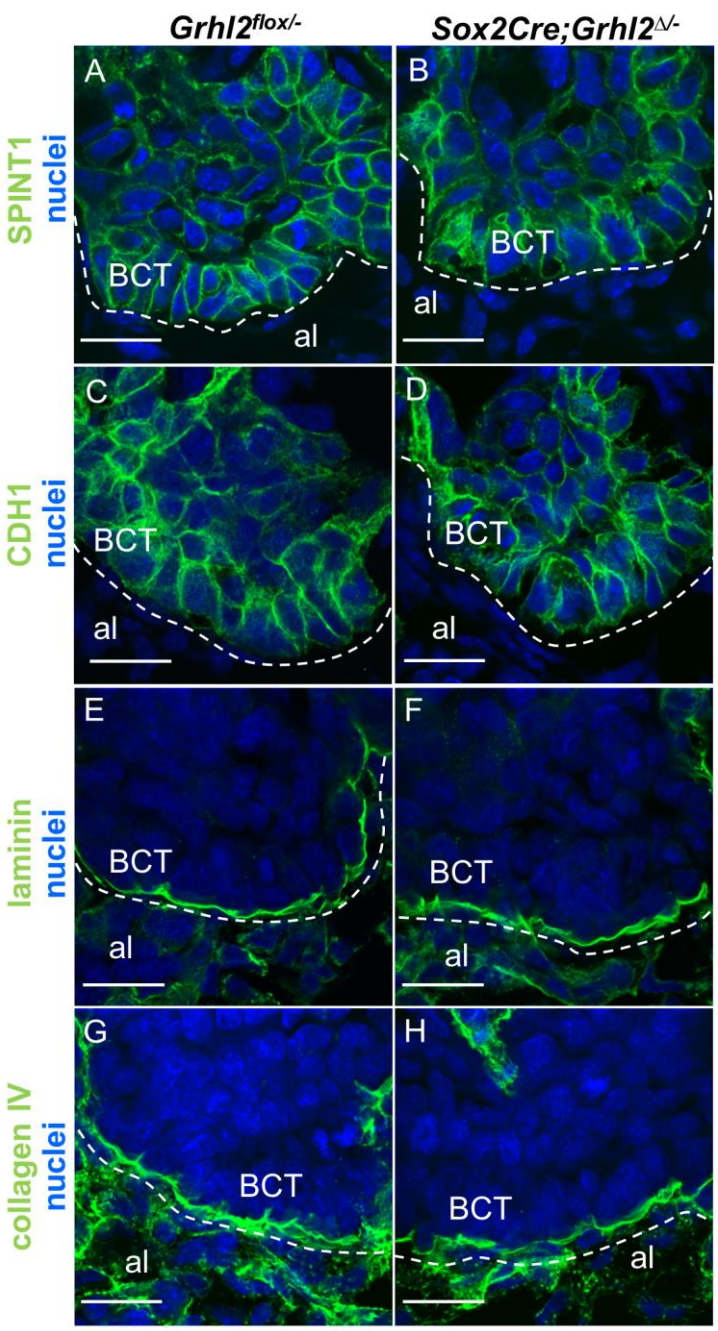

Fig. S8. Epiblast-specific deletion of *Grhl2* using *Sox2Cre* does not induce alterations in SPINT1 and CDH1 expression in BCT cells and preserves continuous basement membranes at the chorioallantoic interface. SPINT1 expression levels (A, B), CDH1 expression levels (C, D) as well as laminin (E,F) and collagen IV deposition (G, H) in BCT cells at the chorioallantoic interface (dashed lines) of *Sox2Cre;Grhl2*$^{\Delta/-}$ embryos (B,D,F,H) are identical to that of their control *Grhl2*$^{flox/-}$ littermates (A,C,E,G). Scale bar: 25 μm. al, allantois. Related to Fig. 3.

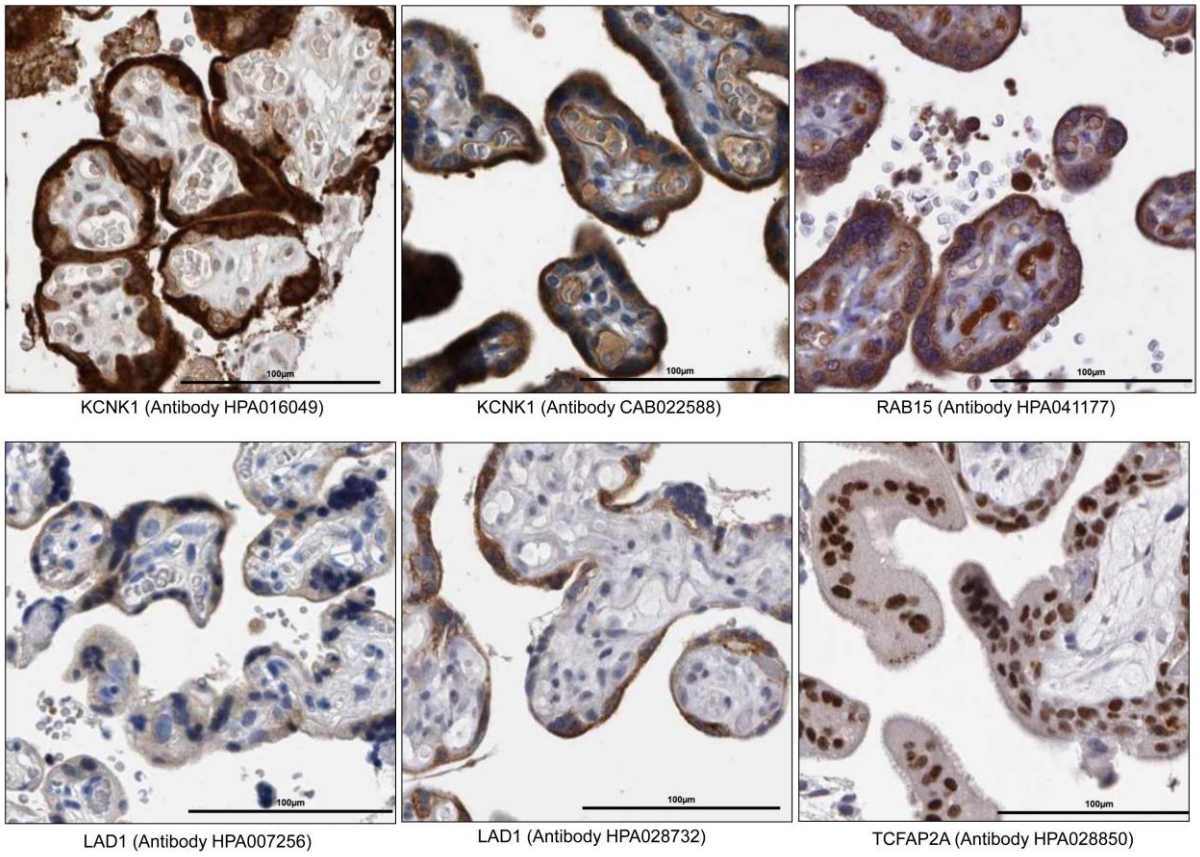

Fig. S9. Placental expression of proteins encoded by human orthologs of the *Grhl2* target gene set. Expression of the indicated proteins was identified in placenta sections from the Human Protein Database (Uhlen et al., 2010) (http://www.proteinatlas.org/). Protein name and antibody identifier (according to the Human Protein Atlas) are shown below each image. Note that all proteins are expressed in villous cytotrophoblasts and/or adjacent syncytiotrophoblasts in a domain similar to the GRHL2 expression domain. Scale bar: 100 µm. Related to Fig. 7.

Supplementary Tables

Table S1. *Grhl2* is crucial for embryonic survival in mice. Time course of lethality in mice resulting from intercrosses of *Grhl2*$^{+/lacZ4}$ and *Grhl2*$^{+/lacZ1}$ mice. Up to E11.5 the distribution of genotypes showed approximately Mendelian ratios (*Grhl2*^{lacZ4}: 20 % +/+, 54 % +/-, 26 % -/-; *Grhl2*^{lacZ1}: 27 % +/+, 44 % +/-, 29 % -/-). No *Grhl2*$^{-/-}$ embryos were found after E11.5 in the offspring of *Grhl2*^{lacZ4} and *Grhl2*^{lacZ1} intercrosses. E, embryonic day; P, postnatal day. Related to Fig. 2.

Strain	Stage	Number of mice (litter)	*Grhl2*$^{+/+}$	*Grhl2*$^{+/-}$	*Grhl2*$^{-/-}$
Grhl2$^{+/lacZ4}$ x *Grhl2*$^{+/lacZ4}$	E7.5	14 (2)	3	7	4
	E8.5	31 (3)	6	16	9
	E9.5	113 (12)	22	63	28
	E10.5	14 (2)	3	8	3*
	E11.5	16 (2)	4	7	5†
	E14.5	5 (1)	0	5	0
	P21	68	23	45	0
Grhl2$^{+/lacZ1}$ x *Grhl2*$^{+/lacZ1}$	E8.5	20 (2)	5	8	7
	E9.5	39 (5)	12	17	10
	E10.5	7 (1)	1	4	2*
	E18.5	8 (1)	4	4	0
	P21	51	19	32	0

*embryos developmentally retarded, †embryos dead

Table S2. Genes downregulated in *Grhl2*$^{-/-}$ (KO) versus control placentas (WT) at both E7.5 and E9.5 identified by microarray analysis. The top 150 genes for each time-point were considered. Fold rank indicated as WT/KO, *P*-values of log2 transformation < 0.05, gene symbols according to Illumina resource file apart from GRHL2 core target gene set. Genes in bold type display genomic GRHL2 association based on at least one GRHL2 binding peak in placental extracts (gene body ± 2 kb). Related to Fig. 4.

		E7.5				E9.5			
Probe ID	Gene name	Average WT	Average KO	Fold change (WT/KO)	Log2 *P*	Average WT	Average KO	Fold change (WT/KO)	Log2 *P*
ILMN_1246392	***Prom2***	**224.6**	**71.1**	**3.2**	**0.0010**	**1055.5**	**96.0**	**11.0**	**0.0047**
ILMN_2919393	***Tmem54***	**154.1**	**76.8**	**2.0**	**0.0040**	**500.2**	**106.0**	**4.7**	**0.0002**
ILMN_2846026	*Rhox4d*	113.8	79.5	1.4	0.0339	1108.2	308.1	3.6	0.0024
ILMN_1227260	***Lad1***	**114.0**	**74.5**	**1.5**	**0.0050**	**546.0**	**200.4**	**2.7**	**0.0068**
ILMN_1257070	*Grhl2*	127.5	74.3	1.7	0.0254	281.5	104.2	2.7	0.0128
ILMN_1259206	*Hrc*	111.8	86.1	1.3	0.0287	703.2	271.5	2.6	0.0051
ILMN_1243939	*9530027K23Rik*	109.0	82.7	1.3	0.0130	818.7	325.1	2.5	0.0017
ILMN_1260582	*LOC280487*	314.8	251.0	1.3	0.0175	2221.9	906.9	2.4	0.0225
ILMN_1217009	***Rab15***	**924.2**	**499.0**	**1.9**	**0.0003**	**4546.8**	**1888.4**	**2.4**	**0.0246**
ILMN_2502226	*Utf1*	159.1	92.4	1.7	0.0032	558.7	236.2	2.4	0.0179
ILMN_2717099	*Irx2*	143.4	89.5	1.6	0.0222	334.0	157.4	2.1	0.0250
ILMN_2859192	*Trpm5*	123.6	85.9	1.4	0.0070	364.6	175.0	2.1	0.0002
ILMN_2602938	***Smpdl3b***	**284.8**	**190.2**	**1.5**	**0.0178**	**1368.1**	**704.7**	**1.9**	**0.0110**
ILMN_1251706	***1600014K23Rik***	**120.1**	**83.6**	**1.4**	**0.0012**	**3820.5**	**2060.4**	**1.9**	**0.0165**
ILMN_1226661	***Ldoc1***	**290.6**	**168.5**	**1.7**	**0.0472**	**2752.4**	**1498.3**	**1.8**	**0.0088**
ILMN_1220726	*Satb1*	637.0	439.4	1.4	0.0140	1647.9	923.8	1.8	0.0063
ILMN_2615917	***Tex19.1***	**420.6**	**208.4**	**2.0**	**0.0126**	**5046.5**	**2838.6**	**1.8**	**0.0407**
ILMN_2538597	*LOC386405*	241.0	171.7	1.4	0.0066	1027.8	579.9	1.8	0.0197
ILMN_1220650	*1600012P17Rik*	124.9	69.8	1.8	0.0184	2829.7	1614.7	1.8	0.0001
ILMN_3009501	***Kcnk1***	**180.9**	**139.1**	**1.3**	**0.0161**	**608.4**	**348.7**	**1.7**	**0.0000**
ILMN_2518197	***Tnk1***	**78.6**	**66.5**	**1.2**	**0.0303**	**273.1**	**160.9**	**1.7**	**0.0162**
ILMN_1225712	*Iap*	1944.6	1350.4	1.4	0.0263	20243.4	12036.5	1.7	0.0447
ILMN_1229393	*LOC100040016*	83.4	65.3	1.3	0.0103	132.4	79.6	1.7	0.0421
ILMN_2648169	*Sfn*	153.4	115.9	1.3	0.0317	506.7	304.9	1.7	0.0061
ILMN_2835771	***Plac1***	**2125.8**	**1149.5**	**1.8**	**0.0233**	**11872.3**	**7177.7**	**1.7**	**0.0183**
ILMN_2637094	*Pcsk6*	230.0	141.3	1.6	0.0182	2821.6	1750.1	1.6	0.0113
ILMN_2764846	***Tcfap2a***	**350.7**	**187.7**	**1.9**	**0.0042**	**371.6**	**234.5**	**1.6**	**0.0307**
ILMN_1221585	*D030026A21Rik*	165.3	134.4	1.2	0.0456	1293.4	823.3	1.6	0.0442
ILMN_2629335	*Nxf7*	455.9	269.6	1.7	0.0393	1135.5	730.7	1.6	0.0335
ILMN_2673776	*E2f2*	204.8	171.8	1.2	0.0032	406.6	263.5	1.5	0.0005
ILMN_2837779	*Trpv2*	258.7	188.6	1.4	0.0266	1791.2	1175.6	1.5	0.0271
ILMN_1237186	***Spint1***	**413.1**	**329.5**	**1.3**	**0.0092**	**2628.9**	**1733.9**	**1.5**	**0.0432**
ILMN_2588474	*Homer2*	848.9	608.8	1.4	0.0158	3343.3	2212.5	1.5	0.0299

Table S3. Top overlapping gene ontology terms (*P*<0.05) for genes displaying GRHL2 association based on placental ChIP-seq data (gene body ± 2 kb) and for the intersection of the top 150 downregulated genes in E7.5 and E9.5 *Grhl2*$^{-/-}$ versus control placentas as determined by microarray analysis. GO terms with less than four ancestor terms, less than two or more than 1000 genes in term and less than two target genes in term have been removed. Gene ontology was performed using HOMER. Related to Fig. 4.

Top overlapping ontology terms of ChIP-seq- and microarray data								
		ChIP-seq				Microarray		
Term	Name	*P*-value	Genes in term	Target genes in term	Gene names	*P*-value	Genes in term	Target genes in term
GO:0060429	epithelium development	0,0000	548	104	Shroom3,Tfap2c,Rbm15,Car2,Smad3,Spint1,Elf5,Map3k7,Esr1,Evpl,Epb4.1l5,Mesp1,Dag1,Gatad2a,Igf1r,Psen1,Kif26b,Pard3,Gpc3,Stat6,Kazn,Upk2,Map2k1,Tead2,Sema3c,Mtss1,Met,Hhip,Ift88,Tsg101,Cecr2,Ovol2,Nckap1,Psap,Zfp568,Tek,Tgm3,Trp63,Ncoa3,Prlr,Bmpr2,Egfr,Tfap2a,Numa1,Myo1e,Tgfbr3,Fras1,Tgm1,Numb,Hs2st1,Ppp3r1,Notch2,Nodal,Ctnnd1,Dlc1,Fzd7,Tmem67,Irf6,Eya1,Wnt7b,Rxra,Dlg1,Pxn,Frem2,B4galt1,Car9,Tgm2,Upk1a,Tead1,Hdac5,Lrp5,Nfib,Jak2,Jup,Trim71,Grhl2,Ryr2,Tfap2b,Phactr4,Lama1,Celsr1,Src,Kdm2b,F11r,Dsg4,Vasp,Dsp,Smad2,Pbx1,Egf,Dlg3,C2cd3,Rac1,Ctsh,Lamb2,Sema5a,Fgfr1,Hectd1,Pde4d,Mir203,Pde2a,Ski,Pml,Pou2f3	0,0052	4	Sfn,Tfap2a,Grhl2,Spint1
GO:0002009	morphogenesis of an epithelium	0,0000	372	70	Tfap2c,Shroom3,Rbm15,Car2,Smad3,Spint1,Map3k7,Esr1,Epb4.1l5,Mesp1,Dag1,Gatad2a,Igf1r,Psen1,Kif26b,Pard3,Gpc3,Tead2,Sema3c,Mtss1,Hhip,Met,Cecr2,Ovol2,Nckap1,Zfp568,Tek,Trp63,Ncoa3,Tfap2a,Egfr,Fras1,Hs2st1,Ppp3r1,Notch2,Nodal,Ctnnd1,Dlc1,Tmem67,Eya1,Wnt7b,Dlg1,Pxn,Frem2,B4galt1,Car9,Tgm2,Tead1,Hdac5,Lrp5,Jup,Trim71,Grhl2,Ryr2,Phactr4,Lama1,Celsr1,Src,Kdm2b,Vasp,Pbx1,Egf,Dlg3,C2cd3,Ctsh,Fgfr1,Sema5a,Hectd1,Ski,Pml	0,0122	3	Tfap2a,Grhl2,Spint1
GO:0048729	tissue morphogenesis	0,0001	489	84	Tfap2c,Shroom3,Rbm15,Car2,Smad3,Spint1,Pkp2,Map3k7,Esr1,Tcf7l1,Epb4.1l5,Mesp1,Twsg1,Mylk,Gatad2a,Dag1,Igf1r,Psen1,Kif26b,Pard3,Gpc3,Prkaca,Tead2,Sema3c,Mtss1,Hhip,Met,Cecr2,Ovol2,Nckap1,Smad1,Zfp568,Tek,Trp63,Ncoa3,Bmpr2,Tfap2a,Egfr,Tgfbr3,Fras1,Hs2st1,Ppp3r1,Notch2,Nodal,Ctnnd1,Dlc1,Tmem67,Eya1,Wnt7b,Rxra,Dlg1,Pxn,Frem2,B4galt1,Car9,Tgm2,Tead1,Hdac5,Lrp5,Jup,Grhl2,Trim71,Ryr2,Phactr4,Lama1,Celsr1,Src,Kdm2b,Vasp,Atp7a,Macf1,Dsp,Egf,Smad2,Pbx1,Dlg3,C2cd3,Ctsh,Fgfr1,Sema5a,Hectd1,Ski,Zfpm1,Pml	0,0251	3	Tfap2a,Grhl2,Spint1
GO:0030855	epithelial cell differentiation	0,0004	232	44	Tfap2c,Shroom3,Rxra,B4galt1,Elf5,Esr1,Upk1a,Evpl,Epb4.1l5,Mesp1,Nfib,Pard3,Kazn,Upk2,Lama1,Map2k1,F11r,Dsg4,Mtss1,Ift88,Tsg101,Dsp,Psap,Rac1,Tgm3,Trp63,Prlr,Lamb2,Bmpr2,Tfap2a,Numa1,Myo1e,Tgm1,Numb,Pde4d,Pde2a,Ppp3r1,Mir203,Ctnnd1,Fzd7,Irf6,Pou2f3,Eya1,Wnt7b	0,0364	2	Sfn,Tfap2a
GO:0043588	skin development	0,0045	58	14	Atp8a2,Ovol1,Tfap2c,Tfap2a,Atp7a,Psen1,Jup,Fras1,Pdgfa,Dsp,Tcf7l1,Irf6,Tgm3,Trp63	0,0026	2	Sfn,Tfap2a
GO:0014020	primary neural tube formation	0,0058	78	17	Tead2,Kdm2b,Shroom3,Vasp,Cecr2,Ovol2,Nckap1,Gatad2a,Tfap2a,Trim71,Grhl2,Hectd1,Ski,Phactr4,Nodal,Dlc1,Celsr1	0,0046	2	Tfap2a,Grhl2
GO:0009790	embryo development	0,0088	939	130	Etl4,Tfap2c,Shroom3,Rbbp8,Elf3,Smad3,Spint1,Map3k7,Prkdc,Gata2,Tcf7l1,Hspg2,Twsg1,Tfeb,Ssbp3,Psen1,Chd7,Psmc3,Satb2,Bcr,Tenm4,Gpc3,Foxp2,Cdh23,Map2k1,Tead2,Cecr2,Ovol2,G2e3,Nckap1,Smad1,Mecp2,Col4a3bp,Trp63,E4f1,Bmpr2,Mll1,Tfap2a,Egfr,Myo1e,Foxk1,Zmiz1,Notch2,Nodal,Tdgf1,Ncor2,Eya1,Clic5,Wnt7b,Mir96,Rxra,Dlg1,Tead1,Mbd3,Jup,Tanc2,Ryr2,Hsd17b2,Chst11,Foxp1,Ppap2b,Vasp,Nipbl,Inpp5b,Smad2,Pbx1,Rac1,Psmc4,Fgfr1,Lmbr1,Gtf2ird1,Tjp1,Plac1,Gab1,Keap1,Efna1,Mesp1,Epb4.1l5,Abcg2,Gatad2a,Abi1,Apba1,Rictor,Ppp1r13l,Mkl2,Tet3,Prkaca,Hoxd3,Ift88,Supt20,Kif16b,Rab14,Mdfi,Zfp568,Plcg1,Bcl2l1,Chrna9,Lrp4,Tgfbr3,Hdac1,Dab2,Hs2st1,Lims1,Dlc1,Fzd7,Ell,Gna12,Ankrd11,Myh9,Gnaq,Lrp5,Hopx,Trim71,Grhl2,Cubn,Zfat,Phactr4,Dnmt3a,Celsr1,Kdm2b,Pik3cb,Macf1,Runx2,Dscaml1,C2cd3,Hmx2,Kif1b,Hectd1,Ski,Zfpm1	0,0066	5	Tfap2a,Plac1,Grhl2,Pcsk6,Spint1
GO:0008544	epidermis	0,0121	195	33	Tfap2c,Fa2h,Pdgfa,Gab1,Atp2c1,Tcf7l1	0,0020	3	Satb1,Sfn,Tf

	development				,Evpl,Psen1,Jup,Mreg,Edar,Kazn,Celsr1,Map2k1,Atp8a2,Dsg4,Atp7a,Tsg101,Dsp,Tgm3,Trp63,Lrp4,Ovol1,Tfap2a,Zdhhc21,Egfr,Fras1,Tgm1,Hdac1,Tfdp1,Ctnnd1,Irf6,Pou2f3			ap2a
GO:0035148	tube formation	0,0128	118	22	Tead2,Kdm2b,Shroom3,Vasp,Cecr2,Ovol2,Nckap1,Map3k7,Tgm2,Gatad2a,Tfap2a,Grhl2,Trim71,Hectd1,Hs2st1,Dab2ip,Nodal,Ski,Phactr4,Dlc1,Edar,Celsr1	0,0103	2	Tfap2a,Grhl2
GO:0006812	cation transport	0,0133	640	91	Slc23a2,Slc22a4,Anxa6,Atp5s,Piezo1,Park2,Kcnma1,Cacna1d,Syk,Slc39a8,Slc11a1,Atp2b4,Cacnb4,Slc9b1,Calcrl,Adra1a,Psen1,Slc24a6,Atp2c2,Piezo2,Vdac1,Nfatc1,Kcnd3,Cdh23,Slc12a8,Atp8a2,Stim1,Armc1,Slc10a7,Ibtk,Uqcr11,Kcnip3,Grin2a,Plcg1,Slc40a1,Chrna9,Kcnq1,Atp8b1,Slc20a2,Camk2d,Slc10a6,Atp9a,Kcnn3,Lmtk2,Kcnj16,Cltc,Slc6a20a,Atp6v1d,Slc39a1,Atp10a,Abcc1,Kcnb2,Slc38a4,Nipa1,Atp2c1,Scnn1a,Atp1a1,Kcnj6,Cox7a2l,Dnm2,Slc39a11,Kcnk1,Slc9a2,Slc9a1,Atp6v1c2,Tcn2,Itpr1,Ryr2,Kcnh6,Sfxn5,Atp11a,Atp9b,Trpm4,Scn7a,Prkce,Slc5a1,Zdhhc17,Cacna1c,Atp7a,Tusc3,Scara5,Slc28a3,Trpc6,Cacna2d1,Cnnm2,Atp6v1g1,Slc9a3r1,Cacna1s,Kcnj15,Slc30a4,Tmem66	0,0494	3	Kcnk1,Trpv2,Trpm5
GO:0016331	morphogenesis of embryonic epithelium	0,0155	134	24	Tead2,Kdm2b,Shroom3,Vasp,Cecr2,Ovol2,Nckap1,Map3k7,Zfp568,Epb4.1l5,Trp63,Tfap2a,Gatad2a,Jup,Grhl2,Trim71,Hectd1,Hs2st1,Nodal,Phactr4,Ski,Dlc1,Celsr1,Wnt7b	0,0131	2	Tfap2a,Grhl2
GO:0030001	metal ion transport	0,0162	480	70	Slc23a2,Slc22a4,Anxa6,Kcnma1,Cacna1d,Slc39a8,Slc11a1,Atp2b4,Cacnb4,Calcrl,Adra1a,Psen1,Slc24a6,Atp2c2,Vdac1,Nfatc1,Cdh23,Kcnd3,Slc12a8,Stim1,Armc1,Slc10a7,Ibtk,Kcnip3,Grin2a,Plcg1,Slc40a1,Kcnq1,Slc20a2,Camk2d,Slc10a6,Kcnn3,Lmtk2,Kcnj16,Cltc,Slc39a1,Kcnb2,Slc38a4,Nipa1,Atp2c1,Scnn1a,Atp1a1,Kcnj6,Slc39a11,Dnm2,Kcnk1,Slc9a2,Slc9a1,Tcn2,Itpr1,Ryr2,Kcnh6,Scn7a,Trpm4,Prkce,Zdhhc17,Slc5a1,Cacna1c,Atp7a,Tusc3,Scara5,Slc28a3,Trpc6,Cacna2d1,Cnnm2,Slc9a3r1,Cacna1s,Kcnj15,Slc30a4,Tmem66	0,0239	3	Kcnk1,Trpv2,Trpm5
GO:0009913	epidermal cell differentiation	0,0165	80	16	Tfap2c,Dsg4,Fa2h,Tsg101,Dsp,Evpl,Tgm3,Trp63,Tfap2a,Tgm1,Hdac1,Ctnnd1,Irf6,Kazn,Pou2f3,Map2k1	0,0048	2	Sfn,Tfap2a
GO:0048598	embryonic morphogenesis	0,0166	504	73	Shroom3,Smad3,Spint1,Map3k7,Efna1,Gata2,Hspg2,Epb4.1l5,Mesp1,Twsg1,Gatad2a,Psen1,Chd7,Satb2,Bcr,Tenm4,Gpc3,Prkaca,Cdh23,Hoxd3,Tead2,Ift88,Kif16b,Supt20,Cecr2,Ovol2,Nckap1,Mdfi,Smad1,Zfp568,Trp63,Lrp4,Chrna9,Bmpr2,Tfap2a,Hdac1,Hs2st1,Notch2,Nodal,Tdgf1,Dlc1,Eya1,Clic5,Wnt7b,Mir96,Dlg1,Gna12,Tead1,Gnaq,Lrp5,Jup,Grhl2,Trim71,Ryr2,Chst11,Phactr4,Ppap2b,Celsr1,Kdm2b,Vasp,Nipbl,Macf1,Smad2,Pbx1,Runx2,Dscaml1,C2cd3,Rac1,Fgfr1,Hmx2,Hectd1,Lmbr1,Ski	0,0271	3	Tfap2a,Grhl2,Spint1
GO:0030216	keratinocyte differentiation	0,0167	67	14	Tfap2c,Dsg4,Tfap2a,Tgm1,Tsg101,Dsp,Ctnnd1,Kazn,Evpl,Irf6,Pou2f3,Tgm3,Map2k1,Trp63	0,0034	2	Sfn,Tfap2a
GO:0060606	tube closure	0,0177	74	15	Tead2,Kdm2b,Shroom3,Tfap2a,Vasp,Gatad2a,Grhl2,Trim71,Cecr2,Hectd1,Nckap1,Phactr4,Ski,Dlc1,Celsr1	0,0042	2	Tfap2a,Grhl2
GO:0009792	embryo development ending in birth or egg hatching	0,0191	602	85	Etl4,Tfap2c,Shroom3,Rbbp8,Elf3,Smad3,Spint1,Gab1,Map3k7,Prkdc,Keap1,Gata2,Hspg2,Abcg2,Epb4.1l5,Tfeb,Gatad2a,Abi1,Ssbp3,Psen1,Apba1,Chd7,Psmc3,Satb2,Mkl2,Map2k1,Hoxd3,Tead2,Ift88,Cecr2,Ovol2,G2e3,Nckap1,Mdfi,Zfp568,Plcg1,Bcl2l1,Col4a3bp,Tfap2a,Egfr,Myo1e,Tgfbr3,Lims1,Zmiz1,Dab2,Notch2,Nodal,Tdgf1,Dlc1,Ncor2,Eya1,Wnt7b,Ell,Rxra,Dlg1,Gna12,Ankrd11,Myh9,Mbd3,Hopx,Tanc2,Grhl2,Trim71,Hsd17b2,Cubn,Chst11,Foxp1,Phactr4,Zfat,Celsr1,Kdm2b,Vasp,Nipbl,Inpp5b,Smad2,Pbx1,Runx2,Dscaml1,C2cd3,Psmc4,Fgfr1,Hectd1,Ski,Tjp1,Plac1	0,0073	4	Tfap2a,Plac1,Grhl2,Spint1
GO:0043009	chordate embryonic development	0,0198	595	84	Etl4,Tfap2c,Shroom3,Rbbp8,Elf3,Smad3,Spint1,Gab1,Map3k7,Prkdc,Keap1,Gata2,Hspg2,Epb4.1l5,Tfeb,Gatad2a,Abi1,Ssbp3,Psen1,Apba1,Chd7,Psmc3,Satb2,Mkl2,Map2k1,Hoxd3,Tead2,Ift88,Cecr2,Ovol2,G2e3,Nckap1,Mdfi,Zfp568,Plcg1,Bcl2l1,Col4a3bp,Tfap2a,Egfr,Myo1e,Tgfbr3,Lims1,Zmiz1,Dab2,Notch2,Nodal,Tdgf1,Dlc1,Ncor2,Eya1,Wnt7b,Ell,Rxra,Dlg1,Gna12,Ankrd11,Myh9,Mbd3,Hopx,Tanc2,Grhl2,Trim71,Hsd17b2,Cubn,Chst11,Foxp1,Phactr4,Zfat,Celsr1,Kdm2b,Vasp,Nipbl,Inpp5b,Smad2,Pbx1,Runx2,Dscaml1,C2cd3,Psmc4,Fgfr1,Hectd1,Ski,Tjp1,Plac1	0,0070	4	Tfap2a,Plac1,Grhl2,Spint1
GO:0034765	regulation of ion transmembrane transport	0,0250	243	38	Kcnj16,Kcnma1,Plcb1,Cacna1d,Fgf12,Kcnb2,Homer1,Cacnb4,Kcnj6,Kcnk1,Ppargc1a,Ryr2,Trpm4,Scn7a,Reln,Vdac1,Kcnd3,Stim1,Cacna1c,Casq2,Trim27,	0,0038	3	Kcnk1,Trpv2,Trpm5

					Egf,Kcnip3,Plcg1,Clcn3,Trpc6,Dapk1,Kcnq1,Cacna2d1,Ano6,Acsl5,Slc9a3r1,Cacna1s,Kcnj15,Nedd4l,Pla2g6,Clic5,Hk1			
GO:0043269	regulation of ion transport	0,0259	444	64	Kcnma1,Plcb1,Cacna1d,Fgf12,Syk,Mgea5,Cacnb4,Mylk,Il1rn,Ppargc1a,Akt3,Il13,Stk39,Reln,Vdac1,Kcnd3,Stim1,Casq2,Trim27,Kcnip3,Plcg1,Kcnq1,Ano6,Camk2d,Nedd4l,Sptbn4,Clic5,Hk1,Kcnj16,Diap1,Dlg1,Sgk1,Kcnb2,Ptk2b,Homer1,Myh9,Atp1a1,Gnaq,Kcnj6,Chrm1,Kcnk1,Itpr1,Ryr2,Scn7a,Trpm4,Ubash3b,P2ry2,Prkce,Cacna1c,Chrm3,Egf,Rtn4,Clcn3,Dapk1,Trpc6,Cacna2d1,Acsl5,Slc9a3r1,Cacna1s,Plcb4,Kcnj15,Pml,Pla2g6,Tmem66	0,0195	3	Kcnk1,Trpv2,Trpm5
GO:0034762	regulation of transmembrane transport	0,0272	252	39	Kcnj16,Kcnma1,Plcb1,Cacna1d,Fgf12,Kcnb2,Homer1,Cacnb4,Kcnj6,Kcnk1,Ppargc1a,Ryr2,Trpm4,Scn7a,Reln,Vdac1,Kcnd3,Stim1,Cacna1c,Casq2,Trim27,Egf,Kcnip3,Plcg1,Clcn3,Lamtor1,Trpc6,Dapk1,Kcnq1,Cacna2d1,Ano6,Acsl5,Slc9a3r1,Cacna1s,Kcnj15,Nedd4l,Pla2g6,Clic5,Hk1	0,0042	3	Kcnk1,Trpv2,Trpm5
GO:0030198	extracellular matrix organization	0,0311	150	25	Col14a1,Fbln1,Fshr,Atp7a,Olfml2a,Elf3,B4galt1,Spint1,Tnr,B4galt7,Hspg2,Mpzl3,App,Lamb2,Ptk2,Dag1,Tfap2a,Myo1e,Col4a3,Csgalnact1,Col19a1,Thsd4,Rxfp1,Abi3bp,Fbln5	0,0162	2	Tfap2a,Spint1
GO:0001701	in utero embryonic development	0,0357	381	55	Ell,Tfap2c,Rxra,Rbbp8,Elf3,Gna12,Smad3,Spint1,Gab1,Ankrd11,Keap1,Gata2,Myh9,Epb4.1l5,Tfeb,Mbd3,Gatad2a,Hopx,Apba1,Chd7,Tanc2,Grhl2,Psmc3,Cubn,Hsd17b2,Mkl2,Zfat,Foxp1,Map2k1,Ift88,Inpp5b,Ovol2,G2e3,Nckap1,Smad2,Mdfi,Zfp568,Plcg1,C2cd3,Bcl2l1,Col4a3bp,Psmc4,Egfr,Fgfr1,Myo1e,Tgfbr3,Zmiz1,Dab2,Notch2,Nodal,Tdgf1,Tjp1,Plac1,Ncor2,Wnt7b	0,0130	3	Plac1,Grhl2,Spint1
GO:0001890	placenta development	0,0382	131	22	Rxra,Hsp90ab1,Met,Rbm15,Spint1,Gab1,Ovol2,Mdfi,Zfp568,Gata2,Prdx3,Tfeb,Egfr,Hsd17b2,Pbrm1,Notch2,Nodal,Birc2,Zfat,Plac1,Map2k1,Wnt7b	0,0125	2	Plac1,Spint1
GO:0001558	regulation of cell growth	0,0399	290	43	Caprin2,Wisp2,Col14a1,Hrg,Sgk1,Map2k5,Adam17,Smad3,Ptprj,Tnr,Gsk3a,Usp47,Ptk2b,Akap6,Cdh13,Rab11a,Eaf2,Ptk2,Slc9a1,Psrc1,Ppp1r9b,Dab2ip,Gas2l1,Ddx3x,Fbp1,Dscam,Osgin1,Cda,Tsg101,Mul1,Sema4d,Tnk1,Rtn4,Ncoa3,Bmpr2,Sh3bp4,Foxk1,Hspa1b,Dab2,Sertad2,Pml,Kif26a,Enpp1	0,0062	3	Sfn,Trpv2,Tnk1
GO:0072175	epithelial tube formation	0,0402	110	19	Tead2,Kdm2b,Shroom3,Vasp,Cecr2,Ovol2,Nckap1,Map3k7,Gatad2a,Tfap2a,Grhl2,Trim71,Hectd1,Hs2st1,Ski,Phactr4,Nodal,Dlc1,Celsr1	0,0090	2	Tfap2a,Grhl2
GO:0001838	embryonic epithelial tube formation	0,0402	110	19	Tead2,Kdm2b,Shroom3,Vasp,Cecr2,Ovol2,Nckap1,Map3k7,Gatad2a,Tfap2a,Grhl2,Trim71,Hectd1,Hs2st1,Ski,Phactr4,Nodal,Dlc1,Celsr1	0,0090	2	Tfap2a,Grhl2

Table S4. Primers used for the validation of *neo*^{r} excision in floxed *Grhl2* mice, genotyping of floxed *Grhl2* mice without *neo*^{r} and *Flp* deleter mice, *Sox2Cre* and *R26R-LacZ* mice. Related to Fig. 3.

	Forward primer sequence 5‘ to 3‘	Reverse primer sequence 5‘ to 3‘	PCR product length
floxed exon 4 with *neo*^{r} floxed exon 4 without *neo*^{r} wild-type exon 4	CGTGATATTGCTGAAGAGCTTG CCAGCTCTATCTCCTGAGAG CCAGCTCTATCTCCTGAGAG	TGTGTTCAGATCGGTGACAG TGTGTTCAGATCGGTGACAG TGTGTTCAGATCGGTGACAG	788 bp 683 bp 541 bp
floxed exon 4 wild-type exon 4	CCAACCTTCCCTTTCCATTC CCAACCTTCCCTTTCCATTC	AGAGGACTTGAAGGTCGGAG AGAGGACTTGAAGGTCGGAG	672 bp 564 bp
R26Fki (FLPe) allele	CCCATTCCATGCGGGGTATCG	GCATCTGGGAGATCACTGAG	700 bp
Sox2Cre allele wild-type allele	GCGGTCTGGCAGTAAAAACTATC CTAGGCCACAGAATTGAAAGATCT	GTGAAACAGCATTGCTGTCACTT GTAGGTGGAAATTCTAGCATCATCC	100 bp 324 bp
R26R-lacZ allele wild-type allele	AAAGTCGCTCTGAGTTGTTAT AAAGTCGCTCTGAGTTGTTAT	GCGAAGAGTTTGTCCTCAACC GGAGCGGGAGAAATGGATATG	314 bp 600 bp

Table S5. Primers used for screening of ES cells to generate floxed *Grhl2* mice. Related to Fig. 3.

	Forward primer sequence 5‘ to 3‘	Reverse primer sequence 5‘ to 3‘	PCR product length
Validation of homologous recombination at 5‘ end	ACAAGGAAGGTGAGGATGAG	CTAGTGAGACGTGCTACTTC	2349 bp floxed allele
Validation of homologous recombination at 3‘ end	CCAACCTTCCCTTTCCATTC	AGAGGACTTGAAGGTCGGAG	672 bp floxed allele 564 bp wild-type allele

Table S6. Riboprobes for *in situ* hybridization. Related to Fig. S3.

Target gene	Linearization for anti-sense probe	Polymerase for anti-sense probe	Insert size	Reference
Tpbpa	EcoRI	Sp6	630 bp	Francois Guillemot
Prl3d1	HindIII	Sp6	800 bp	Malgorzata Gasperowicza/ James Cross
Prl3b1	HindIII	T7	815 bp	Janet Rossant
Prl2c2	HindIII	T7	800 bp	Janet Rossant
Handl	SalI	T7	1475 bp	James Cross
Gcm1	XhoI	T7	1521 bp	Malgorzata Gasperowicza/ James Cross

Table S7. qPCR primers for expression analysis of the *Grhl2* target gene set. Related to Fig. 5.

Target gene	Forward primer sequence 5' to 3'	Reverse primer sequence 5' to 3'
Spint1	ATGTGCAAGGAATCTCACCGAA	CACAGCGTTCACTGAATGGG
Kcnk1	TCTGTGCTGGAGGATGACTG	TGATGTGAACCAGGTCTTCG
Smpdl3b	CAACACAGGTGCCCCCATAA	TGTACATTCGCCTGCCTCAG
Plac1	GTGTCCTGTGCTGCCCCTCG	GGTGGGCAGCTGCAGTTGGG
Tmem54	GGAGGAGAAGGATGGAAGCG	CAGCACCTTCCGGAACTCAT
Prom2	CCTCGTCTTCGTCACTTTCC	TCCAGGTGCTTATCCAGGTC
Ldoc1	CGCCTTTTCATTCCAACCCC	ATCGCTGGAACTCCGAACAG
Lad1	AGAAACACCCTTAACCCGCA	CAGACGCAGATTCTCCTTTCG
Rab15	GATGTGCTGTTCCGGCTACT	GCTCGCCGATAGTACTGCTT
Tnk1	CCCATCACTATCATTGAGGGCA	ATCTTCGTTCTGTGGCTCCG
1600014K23Rik	TGACCCTTGGGAGAATTGCC	GCAGAAGGCTCTGGTTGAGT
Actb	CTAAGGCCAACCGTGAAAAG	TCTCAGCTGTGGTGGTGAAG
Tex19.1	CCATGGGGAACAGACGAAGA	ACATAAAGGGACCCCAATCCC
Grhl2	ACCATCGGGAACATTGAAGA	TCCGGTCCTCTGTAGGTTTG
Tfap2a	CATCGAGGACGTCCCGCACG	TCCCTGGCTAGGTGGACGGC

Table S8. ChIP qPCR primer sequences for validation of the GRHL2 ChIP-seq peak regions. Related to Fig. 5.

Target gene	Forward primer sequence 5' to 3'	Reverse primer sequence 5' to 3'
Spint1	ATCTCCTCAGCCCTGGTTTG	GAGCCAGTTGGACAGGAGTT
Plac1	ATGGTCAGACCCAGGGAAGA	TAGGAAACCGCTGCAGAACC
Prom2	GGCCGTGCATCCTTCTGTAG	GGAGCCCAAACCTGTCGG
Tmem54	CGATGGAGACCCCTTAGAGC	CAGGCCGCCCTCGTTC
Tcfap2a	GCGGGCTTAGAGTTGTCTGA	CTGGTTGTCGGAACAAGCG
Ldoc1	TGCTCTGAAACTCACTTTGGC	AGGGACCTGGAAAATCGCTG
Tex19.1	CAGAGGAACGTTGCTACACCA	ATCAGTGAGCAGCATCGCAG
Kcnk1	CAACATCACCCAGGCCAGT	TGTCTATGGTGGAGGAGGGAT
Tnk1	ACTCTGCTTTCCTCATAGCCC	GTAAGCCAAAATCTGGCCCC
Smpdl3b	TCCTCCAATCAAGCGCACG	AGTTATCCTTGGCGGATGGC
1600014K23Rik	ATCTGTAGCGCACTCCAAAGTT	CCTGGAAAGCCAATCACAGGAA
Lad1-peak1	AGCTCTTGGGTTTCTGCCG	GAACCCAAAGATCGGGGTCA
Lad1-peak2	CAGCCCCACCTAGTGGATAAG	GGGTTGTGACAGGCCAATCT
Rab15	TAGGCTCACCTGGTTCTCCG	CCCCTCCCCACTCTGAAGAA
Control locus	CGTGGCTCATGTGTCAACTAA	CGATGGGACATGGTAGTGTCT

Supplementary Experimental Procedures

Microarray analysis

Total RNA from E7.5 trophectoderm-derived tissues and E9.5 placenta was isolated using the RNeasy Mini Kit (Qiagen, Hilden, Germany) according to manufacturer's instructions including treatment with RNase-free DNase I (Qiagen, Hilden, Germany). Subsequently, RNA was amplified for hybridization with Illumina® MouseWG-6 v2.0 Expression BeadChips (San Diego, CA, USA) using the Ambion® Illumina® TotalPrep™ RNA Amplification Kit (Life Technologies, Darmstadt, Germany). After quantile normalization of the data, we filtered out the genes with a valid RefSeq ID (referring to the annotation file provided by Illumina; http://www.switchtoi.com/annotationfiles.ilmn) and with a *P*-value of the respective log2-transformed expression values less than 0.05 using Student's t test. For heat-map generation, gene expression values were maximum normalized on a per-gene basis for E7.5 and E9.5, separately.

The publicly deposited data samples from human placenta were downloaded from GEO (http://www.ncbi.nlm.nih.gov/geo/), namely the sets under the following URL's: http://www.ncbi.nlm.nih.gov/sites/GDSbrowser?acc=GDS4037, http://www.ncbi.nlm.nih.gov/sites/GDSbrowser?acc=GDS3467 and http://www.ncbi.nlm.nih.gov/sites/GDSbrowser?acc=GDS2990 (Huuskonen et al., 2008; Mikheev et al., 2008; Founds et al., 2009). For our analysis, we only compared probes with the same Affymetrix ID. Log2 transformed data was re-transformed if necessary. As mentioned in the text, the potential GRHL2 target genes show a high correlation with *Grhl2* itself and among each other. The high correlation coefficients of all targets with *Grhl2* are with a probability of less than 0.01 due to random effects. For this *P*-value, correlation coefficients of all genes from the datasets with *Grhl2* have been calculated. Clearly, taking n genes randomly from the dataset and having m ($m \leq n$) correlation coefficients above a level r0 follows a hypergeometric distribution. Setting r0 to be the minimum correlation coefficient among the core target module and having m=n=12 (plus number of genes and number of genes with a correlation coefficient $\geq$r0), led to the respective *P*-value.

Biocomputational analysis of ChIP sequencing

Following initial quality filtering and genome alignment using Bowtie software (Langmead et al., 2009), we obtained around 30 million aligned reads per experiment. To predict GRHL2-associated genomic regions, we used MACS for peak analysis (Zhang et al., 2008) on GRHL2 ChIP samples and on IgG control ChIP samples as background control (threshold *P*-value $1x10^{-5}$). This yielded 5,282 peaks from mouse placenta. The peaks were ranked according to the intrinsic scores provided by MACS (negative log10 transform of the peak's *P*-value). Motif finding was then performed using MEME (Bailey et al., 2009) in the top 10% of all peaks in a 50 bp window around the peak's summit and optimized for de novo detection of 8-9 bp motifs. Motif enrichment in a given sequence set was done by using MAST (Bailey and Gribskov, 1998) and FIMO (Grant et al., 2011). The resulting GRHL2 motif was subjected to TOMTOM analysis (Bailey et al., 2009) for comparison with known transcription factor recognition matrices. Visualization of the ChIP data was carried out using the Integrative Genome Viewer provided by the Broad Institute (Robinson et al., 2011).

For the functional characterization of the GRHL2 ChIP peak at the 3' end of *Spint1*, we used H3K4me1 and H3K27ac ChIP-seq data on mouse placentas from ENCODE. The respective files can be found under wgEncodeLicrHistonePlacH3k04me1FAdult8wksC57bl6StdPk and wgEncodeLicrHistonePlacH3k27acFAdult8wksC57bl6StdPk. We did not use the provided peak tracks and computed them using MACS with the same parameters as for our own data.

Further analysis and visualization of microarray and ChIP-seq data

After peak finding, we found peak-related genes using the closest method of the bedtools suite (Quinlan and Hall, 2010). The respective gene coordinates were obtained from the refGene table of UCSC table browser (http://genome.ucsc.edu/cgi-bin/hgTables?command=start). Setting a distance threshold of 2 kb produced a list of genes near a ChIP peak area. Analysis of our gene expression data also produced gene lists. We then performed an ID conversion using DAVID to entrez gene ID (Huang da et al., 2009b, a) and a manual conversion of gene names not matched by DAVID using the RefSeqGene web page (http://www.ncbi.nlm.nih.gov/refseq/rsg/). After this, the respective lists were intersected to yield the desired target gene set. All list operations were done by self-written Python

programs. The visualization as well was performed by self-written programs in Python using the matplotlib package (http://matplotlib.org/).

ChIP peak annotation to the respective genomic regions (Promoter/TSS, Intergenic etc.) was done using the HOMER software package (Heinz et al., 2010). Random genomic intervals were generated using the shuffle method in the bedtools suite.

Animals

Mice with a conditional (floxed) *Grhl2* allele were obtained from embryonic stem (ES) cells containing a targeted *Grhl2* gene with the fourth exon flanked by loxP sites (see supplementary Material Fig. S5A). Upstream from the floxed exon 4, a neomycin resistance sequence (*neo*^{r}) flanked by two FRT sites was integrated for positive selection. The targeted ES cell clones were generated by electroporation and integration of the targeted construct into the genome of mouse KV1 ES cells (derived from 129B6 hybrid mice) through homologous recombination. Random integration was reduced by the presence of a diphtheria toxin A (*dta*) cassette at the 5' end of the construct. Following G418 selection, a screening for ES cell clones positive for homologous recombination was carried out by PCR using primers depicted in supplementary Material Table S5. A positive ES cell clone was injected into C57BL/6 blastocysts to generate *Grhl2*$^{flox/+}$ mice via standard procedures. Excision of *neo*^{r} was achieved through breeding of *Grhl2*$^{flox/+}$ mice with Flp deleter mice (Farley et al., 2000). *Grhl2*$^{flox/flox}$ mice were viable and fertile. Breeding of female *Grhl2*$^{flox/flox}$ mice with heterozygous *Grhl2*$^{+/-}$ males carrying the *Sox2Cre* transgene (*Sox2Cre;Grhl2*$^{+/-}$) enabled selective *Grhl2* inactivation in the epiblast-derived mouse embryo corpus and in the epiblast-derived extra-embryonic membranes (amnion, yolk sac, allantois) without impairment of the trophectoderm-derived trophoblast lineages through generating *Sox2Cre;Grhl2*$^{\Delta/-}$ mice (Hayashi et al., 2002). *Grhl2*$^{flox/flox}$ and *Sox2Cre;Grhl2*$^{\Delta/-}$ mice were on a mixed 129/C57BL/6 genetic background. Genotyping was done by PCR with primers indicated in supplementary Material Table S4. For timed pregnancies, breeding females were checked for vaginal plugs in the morning. The plug date was considered as embryonic day 0.5 (E0.5).

Antibodies

The following antibodies were used: anti-GRHL2 (HPA004820, Sigma-Aldrich, Hamburg, Germany, 1:200 (immunofluorescence), 6 µg per immunoprecipitation), anti-cleaved caspase 3 (G7481, Promega, Mannheim, Germany, 1:250), anti-CD71 (MCA1033GA, AbD Serotec/MorphoSys AG, Puchheim, Germany, 1:150), anti-MTP1 (MTP11-A, Alpha Diagnostic, San Antonio, Texas, 1:150), anti-pan-cytokeratin-FITC (F3418, Sigma-Aldrich, Hamburg, Germany, 1:100), anti-laminin (L9393, Sigma-Aldrich, Hamburg, Germany, 1:150), anti-Ki-67 (M7249, Dako, Hamburg, Germany, 1:200), anti-PECAM1 (550274, BD Pharmingen, Heidelberg, Germany, 1:100), anti-TCFAP2C (sc-8977 (H-77), Santa Cruz, Heidelberg, Germany, 1:200), anti-collagen IV (AB756, Millipore Corporation, Billerica, MA, 1:150), anti-CDH1 (3195S, New England Biolabs, Frankfurt am Main, Germany, 1:250), anti-SPINT1 (AF1141, R&D Systems Inc, Wiesbaden-Nordenstadt, Germany, 1:50), anti-ITGA6 (MCA699GA, AbD Serotec/MorphoSys AG, Puchheim, Germany, 1:150), rabbit Cldn4 (36-4800, Life Technologies GmbH, Darmstadt, Germany, 1:250), rabbit IgG (011-000-003, Jackson ImmunoResearch, Newmarket, UK, 6 µg per immunoprecipitation).

Immunofluorescence staining and confocal microscopy

Cryo-embedded tissues were cut into 16 µm thick sections and subjected to immunofluorescence staining. After incubation of tissue sections in blocking buffer (PBS/1% BSA/0.05% triton-X-100) for 1 hour, primary antibodies were incubated overnight at 4°C. Primary antibodies were detected with secondary antibodies diluted in blocking buffer and labeled by Cy2, Cy3 or Cy5 (Jackson ImmunoResearch, Newmarket, UK). Nuclei were visualized using TO-PRO®-3 iodide (Life Technologies GmbH, Darmstadt, Germany). Fluorescent microscopy was done on an inverted TCS SP5 tandem confocal microscope (Leica Microsystems GmbH, Wetzlar, Germany). For comparing relative intensity of immunofluorescence staining, the z-plane was adjusted for maximal fluorescence intensity, and image acquisition settings were maintained to be identical for all samples.

GRHL2 immunohistochemistry

For immunohistochemistry, we used the EnVision System-HRP (AEC) kit for the use with rabbit primary antibodies (Dako, Hamburg, Germany) according to manufacturer's instructions. Tissues were fixed in PBS/4% PFA for 1 hour at 4°C, dehydrated, embedded in paraffin and cut into 10 µm thick sections. GRHL2 antigen retrieval was done by incubation for 20 minutes at 100°C in 10 mM citrate buffer pH 6.0.

Hematoxylin and Eosin (H&E) staining

Paraffin-embedded tissue was cut into 5 µm thick sections. Before staining, slides were incubated for 30 minutes to 2 hours at 62°C laying upright in a rack to melt off the paraffin wax. After drying for 30 minutes at room temperature tissue sections were dewaxed by incubating two times in toluol for 5 minutes and rehydrated using a descending ethanol series (100% ethanol: 2 x 2 minutes, 96% ethanol: 2 x 2 minutes, 80% ethanol: 1 x 2 minutes, 70% ethanol: 1 x 2 minutes, ddH_2O: 1 x 2 minutes). Tissue sections were then incubated for 2 to 3 minutes in hemalum solution acid according to Mayer and washed for 30 s in tap water for staining of the nuclei. After short incubation in 1% eosin Y/water solution slides were washed again in tap water and covered with glycerin gelatin and cover slip.

Human tissue samples

We included non-laboured placenta samples from complicated and uncomplicated pregnancies delivered by elective Cesarean section at Oslo University Hospital, Oslo, Norway to analyse expression correlation of *GRHL2* and *SPINT1*. The Regional Committee of Medical Research Ethics in Eastern Norway approved the study and informed written consent was obtained from each participant (ref 529-02162). Placental biopsies from a centrally located normally looking cotyledon (from the center of the cotyledon; omitting the maternal surface and fetal membrane tissues) were obtained following Cesarean sections from 56 preeclamptic women and 28 women with normal normotensive and uncomplicated pregnancies.

In situ hybridization

In situ hybridization on placenta tissue sections was carried out as described previously (Hammes et al., 2001; Schmidt-Ott et al., 2007). Riboprobes were produced from the appropriate plasmids (Table S6). Digoxigenin-labeled cRNA was produced using T7 or T3 polymerase as indicated.

RNA extraction, cDNA synthesis and real-time PCR

Total RNA was isolated using RNeasy Mini Kit (Qiagen, Hilden, Germany) according to manufacturer's instructions including treatment with RNase-free DNase I (Qiagen, Hilden, Germany). First-strand cDNA synthesis was carried out from 500 ng of total RNA from each sample as template with the RevertAid™ First Strand cDNA Synthesis Kit (Fermentas/Fisher Scientific, Schwerte, Germany) according to manufacturer's instructions. Real-time PCR was performed using cDNA as template for expression analyses or DNA for ChIP-seq validation, MESA GREEN qPCR MasterMix Plus for SYBR Assay Rox (Eurogentec, Cologne, Germany) and primers at a final concentration of 200 nM each. For primer sequences used for the validation of Illumina microarray results and for the validation of the GRHL2 ChIP-seq peaks see Table S7 and S8, respectively. Relative levels of mRNA expression were normalized for beta-actin mRNA expression for expression analyses or for total input for ChIP experiments and calculated according to the ddCT method. Statistical significance of differences between two groups was analyzed using two-sided Student's t-test.

Electron microscopy

E9.5 placentas were fixed with 3% glutaraldehyde in 0.1 M sodium cacodylate buffer and 2 mM $CaCl_2$ for 24 hours at 4°C. After washing twice in 0.1 M sodium cacodylate buffer for 30 minutes, placentas were post-fixed in 1% osmium tetroxide (OsO_4) in 0.1 M cacodylate buffer for 2 hours. Afterwards, placentas were washed again twice in 0.1 M sodium cacodylate buffer for 30 minutes, respectively. Samples were dehydrated in a graded ethanol series (70% ethanol: 2 x 20 minutes, 90% ethanol: 2 x 20 minutes, 100% ethanol: 2 x 20 minutes) and propylene oxide (2 x 10 minutes) and embedded in Poly/Bed 812^{R} (Polysciences, Eppelheim, Germany). Polymerization was done at 60°C for 2 to 3 days. Ultrathin sections (70 nm) were contrasted with uranyl acetate and lead citrate and examined with a

Morgagni electron microscope (FEI). Digital images were taken with a Morada CCD camera and the iTEM software (Olympus Soft Imaging Solutions GmbH, Münster, Germany).

Analysis of fluorescence intensity

Fluorescence intensity of immunofluorescence-stained tissue sections was analyzed using the image editing software ImageJ. Immunofluorescence images were first converted into grayscale. Then, BCT cells and overlying chorionic trophoblast cells were separately selected using the freeform selection tool and the level of fluorescence in these regions was analyzed. Mean gray values were determined, mean fluorescence of background readings was subtracted and the relative expression levels were calculated and plotted.

Importantly, for comparing different samples, staining procedures of *Grhl2* control and *Grhl2*$^{-/-}$ placenta sections were performed with identical reagents and in parallel. In addition, image acquisition was also done in parallel using identical image acquisition settings and exposure times.

Supplemental References

Bailey, T. L., Boden, M., Buske, F. A., Frith, M., Grant, C. E., Clementi, L., Ren, J., Li, W. W. and Noble, W. S. (2009). MEME SUITE: tools for motif discovery and searching. *Nucleic Acids Res* **37**, W202-W208.

Bailey, T. L. and Gribskov, M. (1998). Combining evidence using p-values: application to sequence homology searches. *Bioinformatics* **14**, 48-54.

Farley, F. W., Soriano, P., Steffen, L. S. and Dymecki, S. M. (2000). Widespread recombinase expression using FLPeR (flipper) mice. *Genesis* **28**, 106-110.

Founds, S. A., Conley, Y. P., Lyons-Weiler, J. F., Jeyabalan, A., Hogge, W. A. and Conrad, K. P. (2009). Altered global gene expression in first trimester placentas of women destined to develop preeclampsia. *Placenta* **30**, 15-24.

Grant, C. E., Bailey, T. L. and Noble, W. S. (2011). FIMO: scanning for occurrences of a given motif. *Bioinformatics* **27**, 1017-1018.

Hammes, A., Guo, J. K., Lutsch, G., Leheste, J. R., Landrock, D., Ziegler, U., Gubler, M. C. and Schedl, A. (2001). Two splice variants of the Wilms' tumor 1 gene have distinct functions during sex determination and nephron formation. *Cell* **106**, 319-329.

Hayashi, S., Lewis, P., Pevny, L. and McMahon, A. P. (2002). Efficient gene modulation in mouse epiblast using a Sox2Cre transgenic mouse strain. *Mech Dev* **119 Suppl 1**, S97-S101.

Heinz, S., Benner, C., Spann, N., Bertolino, E., Lin, Y. C., Laslo, P., Cheng, J. X., Murre, C., Singh, H. and Glass, C. K. (2010). Simple combinations of lineage-determining transcription factors prime cis-regulatory elements required for macrophage and B cell identities. *Mol Cell* **38**, 576-589.

Huang da, W., Sherman, B. T. and Lempicki, R. A. (2009a). Bioinformatics enrichment tools: paths toward the comprehensive functional analysis of large gene lists. *Nucleic Acids Res* **37**, 1-13.

Huang da, W., Sherman, B. T. and Lempicki, R. A. (2009b). Systematic and integrative analysis of large gene lists using DAVID bioinformatics resources. *Nat Protoc* **4**, 44-57.

Huuskonen, P., Storvik, M., Reinisalo, M., Honkakoski, P., Rysa, J., Hakkola, J. and Pasanen, M. (2008). Microarray analysis of the global alterations in the gene expression in the placentas from cigarette-smoking mothers. *Clin Pharmacol Ther* **83**, 542-550.

Langmead, B., Trapnell, C., Pop, M. and Salzberg, S. L. (2009). Ultrafast and memory-efficient alignment of short DNA sequences to the human genome. *Genome Biol* **10**, R25.

Mikheev, A. M., Nabekura, T., Kaddoumi, A., Bammler, T. K., Govindarajan, R., Hebert, M. F. and Unadkat, J. D. (2008). Profiling gene expression in human placentae of different gestational ages: an OPRU Network and UW SCOR Study. *Reprod Sci* **15**, 866-877.

Quinlan, A. R. and Hall, I. M. (2010). BEDTools: a flexible suite of utilities for comparing genomic features. *Bioinformatics* **26**, 841-842.

Robinson, J. T., Thorvaldsdottir, H., Winckler, W., Guttman, M., Lander, E. S., Getz, G. and Mesirov, J. P. (2011). Integrative genomics viewer. *Nat Biotechnol* **29**, 24-26.

Schmidt-Ott, K. M., Masckauchan, T. N. H., Chen, X., Hirsh, B. J., Sarkar, A., Yang, J., Paragas, N., Wallace, V. A., Dufort, D., Pavlidis, P., Jagla, B., Kitajewski, J. and Barasch, J. (2007). beta-catenin/TCF/Lef controls a differentiation-associated transcriptional program in renal epithelial progenitors. *Development* **134**, 3177-3190.

Uhlen, M., Oksvold, P., Fagerberg, L., Lundberg, E., Jonasson, K., Forsberg, M., Zwahlen, M., Kampf, C., Wester, K., Hober, S., Wernerus, H., Bjorling, L. and Ponten, F. (2010). Towards a knowledge-based Human Protein Atlas. *Nat Biotechnol* **28**, 1248-1250.

Zhang, Y., Liu, T., Meyer, C. A., Eeckhoute, J., Johnson, D. S., Bernstein, B. E., Nusbaum, C., Myers, R. M., Brown, M., Li, W. and Liu, X. S. (2008). Model-based analysis of ChIP-Seq (MACS). *Genome Biol* **9**, R137.